Cooling Processes : Main Points

Goldsmith & Langer 1978

① For low $n(H_2)$, $\Lambda^{(A)}/n(A)$ $\propto n(H_2)$, is independent of $X(A)/(dv/dr)$

escape probab.

→ optically thin limit, $\beta = 1$

$$\Lambda(A) \propto X(A)\, n^2(H_2)$$

② for optically thin case, $\Lambda(A) \propto n(H_2)$ long after lower transitions are thermalized

ie get little information on cooling by CO from J=1-0 line if $n > 100$

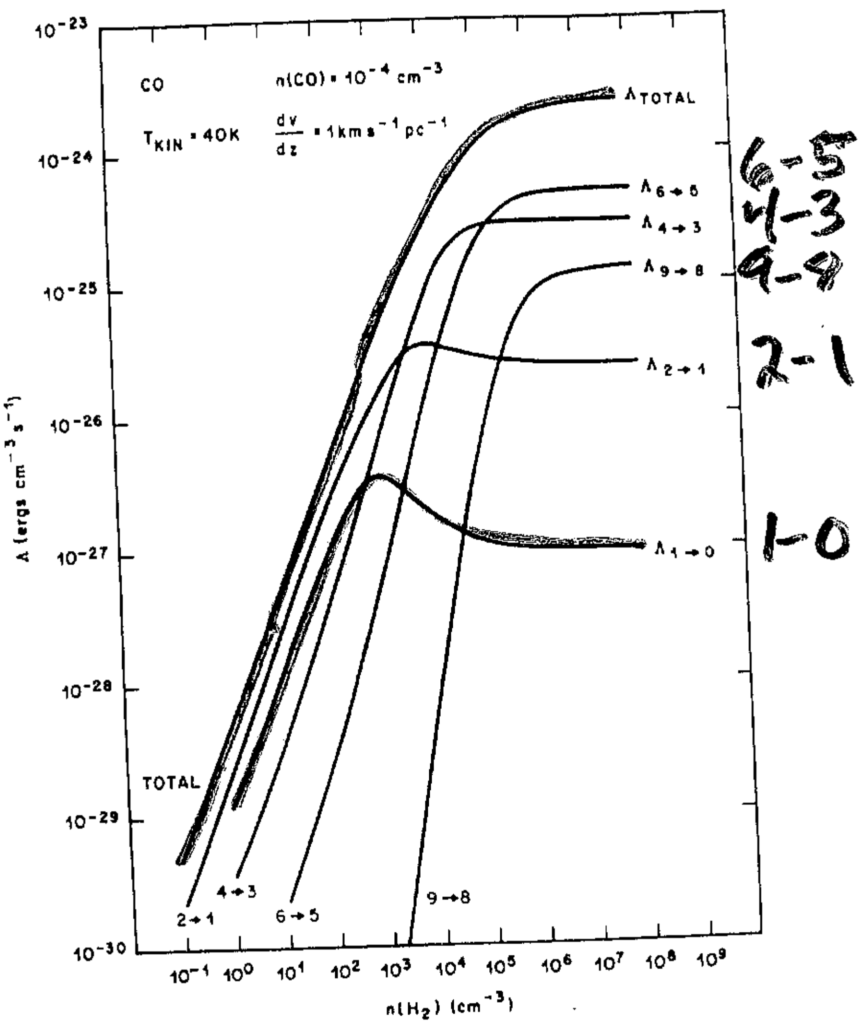

FIG. 1.—Contributions from different transitions to CO cooling at a kinetic temperature of 40 K. The density of CO is chosen to make all transitions optically thin, and is held constant throughout. Note that the total cooling continues to be proportional to $n(H_2)$ long after $\Lambda_{1\to0}$ (which is proportional to $T_{A1\to0}$) has become essentially independent of $n(H_2)$.

most cases (including CO and HCN) this is indicative of the optically thin limit in which the escape probability $\beta \to 1$ for all transitions. In this limit $\Lambda(A) \propto X(A)n^2(H_2)$; this is the regime characteristic of diffuse clouds and is also discussed by de Jong, Chu, and Dalgarno (1975) for carbon monoxide. This behavior of $\Lambda(A)$ can also occur when $\beta \ll 1$ if the collisional de-excitation rate C is much less than the spontaneous decay rate $A_{J\to I}$, as is the case for H_2O. As discussed by Linke *et al.* (1977), in this regime the flux from any individual transition will still be proportional to the

transitions become optically thi
the maximum hydrogen densi
10^7 cm^{-3}.

b) Optically Thic

For thermalized transitions, t
reduces the cooling per molecule
of the Figures (2)–(6), for large
cooling per molecule is inve
$X(A)/(dv/dr)$; thus the cooling
independent of $X(A)$ and propo

Once the opacity in a partic
the cooling must be that of a b
of the size and molecular densi
can be seen to follow from
$\tau \gg 1, \beta \to \tau^{-1}$, and for a single
ν_{IJ} (neglecting, for simplicity,
ation), the cooling rate per uni

$$\Lambda(A)_{IJ} = \frac{A_{J\to I}h\nu_{J}}{\tau}$$

where f_J is the fractional popu
equation (4), we can write

$$\tau_{IJ} = \frac{h[f_J n(A)]}{dv/dr} B_{J\to I}[\mathrm{ex}$$

where $T_* \equiv h\nu_{IJ}/k$ and T_{EX} is
ture of the transition. The usu
the B's and A's (cf. Goldsmit

$$\Lambda(A)_{IJ} = \frac{8\pi h\nu_{IJ}^4}{c^3} [\exp (T_*$$

which has the form of the co
this single transition from a b
T_{EX}.

For intermediate hydroge
thermalize all of the cooling
opacities, the radiation trappi
on the level populations. This
in which the broken line in
would be produced if the exp
the escape probability (eq. [2
level populations n_I and n_J w

3) For optically thick & thermalized transitions, increasing opacity <u>reduces</u> cooling per molecule

$$\Lambda(A)/n(A) \propto (X(A)/(dv/dr))^{-1}$$

why?

$\tau \gg 1 \rightarrow$ cooling is blackbody

$\rightarrow \beta \rightarrow \tau^{-1}$

$$\Lambda(A)_{IJ} = \frac{A_{J\rightarrow I}\, h\nu_{JI}\, [f_J\, n(A)]}{\tau_{IJ}}$$

but $\tau_{IJ} = \dfrac{h\,[f_J\, n(A)]}{dv/dr} B_{J\rightarrow I}\left(e^{\frac{h\nu}{kT_{ex}}}-1\right)$

$$\rightarrow \Lambda(A)_{IJ} = \frac{8\pi h \nu_{IJ}^4}{c^3}\left(e^{\frac{h\nu}{kT_{ex}}}-1\right)^{-1}\frac{dv}{dr}$$

$$\therefore \frac{\Lambda(A)}{n(A)} \propto \left(\frac{X(A)}{dv/dr}\right)^{-1} n(H_2)^{-1}$$

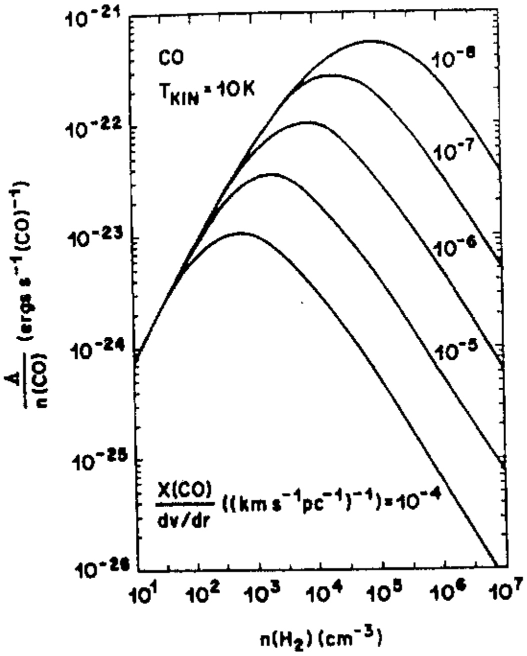

FIG. 2*a*

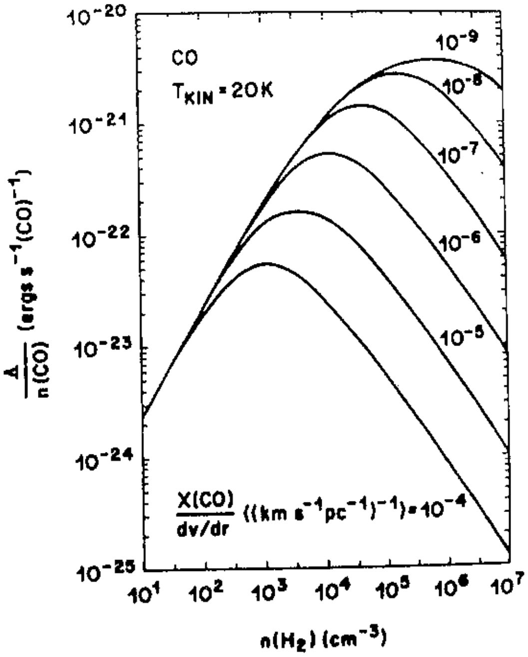

FIG. 2*b*

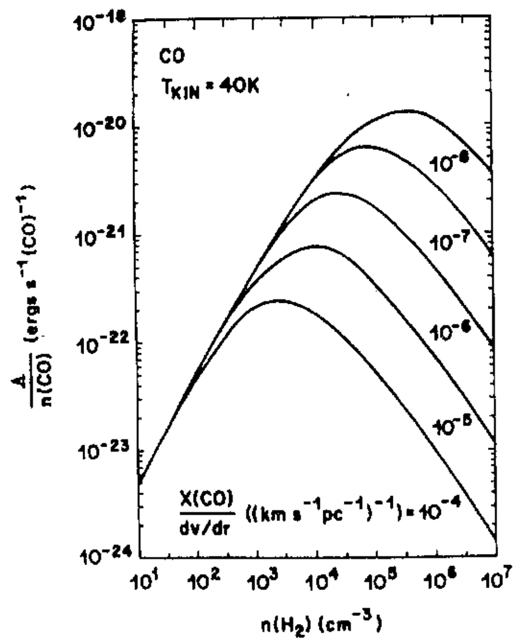

FIG. 2*c*

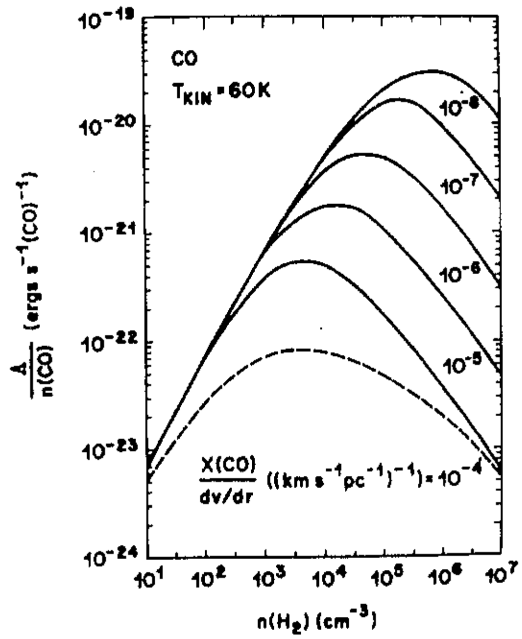

FIG. 2*d*

43

. 2(*a*)–2(*d*).—Cooling per CO molecule as a function of $n(H_2)$ and CO fractional abundance for kinetic temperatures 10 K, 0 K, and 60 K. The broken line in Fig. 2*d* indicates the cooling for $X(CO)/(dv/dr) = 10^{-4}$ (km s^{-1} pc^{-1})$^{-1}$ if the effect of g on the escape probabilities but not on the level populations is taken into account. The trapping reduces the population of ≤ 3 and increases the population of levels $J \geq 4$.

lly thick at any temperature ≥ 10 K. The peak cooling curve as a function of J thus occurs at a value than J^*. Empirically we find that the

10 K, 20 K, 40 K, and 60 K in Figures 2*a*–2*d*. Each figure contains a number of curves parametrized by $X(CO)/(dv/dr)$ with dv/dr in units of km s^{-1} pc^{-1}.

Important molecules

① CO, ^{13}CO, $C^{18}O$

- radiative trapping affects CO, so isotopes can be important at highish densities

② C I

- fine-structure level at 23.4 K
- important at low (10-20K) temperatures

③ O_2

- efficiency comparable to CO
- rotational transitions

④ H_2O

- more important at high temperatures, densities

Total cooling dominated by
^{12}CO for $n < 10^3$
^{13}CO, $C^{18}O$, CI, O_2 30-70% for $n > 10^3$

for CO cooling alone; with the inclusion of various molecular species with greatly differing A-coefficients, however, the total cooling is dependent upon the molecular hydrogen density throughout the range of conditions considered here.

We next shall discuss some of the heating sources that may play a role in determining the thermal balance of dense clouds. The heating rate for each will be calculated and the conditions under which it might contribute significantly to the cloud heating analyzed.

a) Heating Mechanisms

The cooling rates that we have derived can be used to determine the time scale for thermal cooling in interstellar clouds. This time scale is estimated, from the formula $\tau_{th} = 1.5kT[\Lambda/n(H_2)]$ and from the rates in Table 4, to be less than 10^5 years over the range of densities 10^3–10^4 cm^{-3} for $T_{kin} > 8$ K—roughly an order of magnitude less than the free-fall time. This relatively short thermal time scale strongly suggests that there must be a heating source for these objects which maintains them in thermal equilibrium. Several possible sources of heating, which will be discussed below, are cosmic rays, H_2 formation, and gravitational contraction.

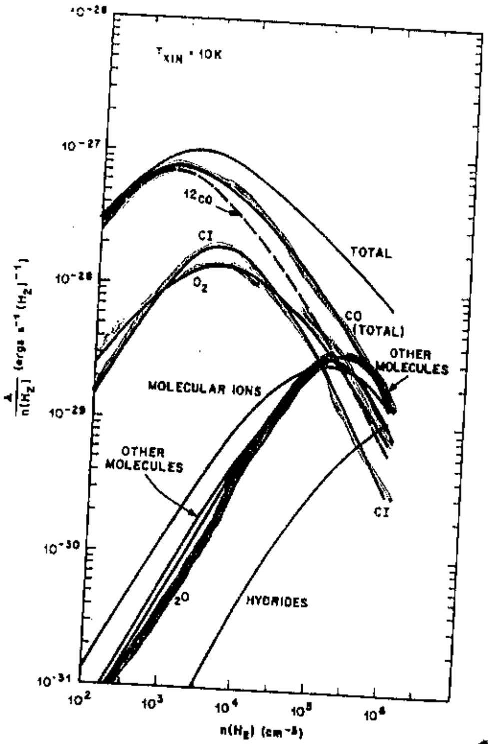

FIG. 7a

— CO
— CI
— O2
— H2O

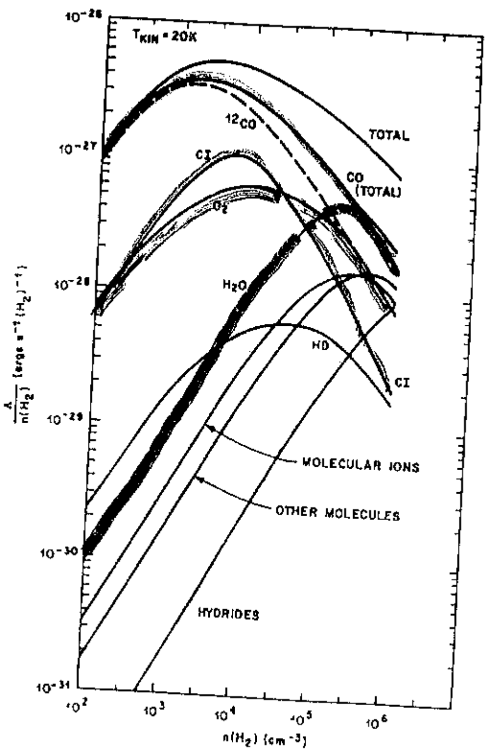

FIG. 7b

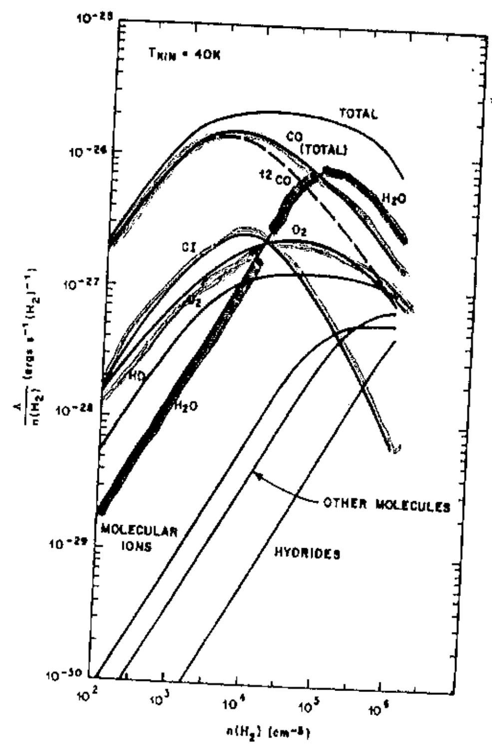

FIG. 7c

FIGS. 7(a)–7(c).—Total cooling per H_2 molecule as a function of H_2 density for kinetic temperatures 10 K, 20 K, and 40 K. The fractional abundance for each species has been taken from Table 3.

Thermal Balance

Cooling timescale $\tau_{th} = 1.5 kT \,[\Lambda / n(H_2)]$

$\lesssim 10^5$ yr

Heating sources

- cosmic rays (ionize H_2)
- H_2 formation (binding energy)
- gravitational contraction
- ambipolar-diffusion (depends on X_e, B)

Clouds with internal heat sources

→ $T > 40K$ → dust heats gas (need $n > 10^5$ for strong coupling)

→ $15 < T < 40K$ (moderate luminosity)

→ need H_2 formation • ambipolar diffusion

Dark clouds (6–15 K, 10^2–10^4 cm^{-3})

- cosmic rays can work (and so can the other 3 mechanisms under certain conditions)

How do we get physical quantities from molecular line observations?

ie T temperature

n density

N column density

τ optical depth

$\frac{[X]}{[H_2]}$ relative abundance

Two very common approximations or models are

(1) LTE "Local Thermodynamic Equilibrium"

(2) LVG "Large Velocity Gradient

(1) LTE

We assume that the level populations of a molecule are given by a single excitation temperature, and that

$$T_{ex} = T_{kin} \quad \text{(kinetic temperature}$$

so $$\frac{N_l}{N_u} = \frac{g_l}{g_u} e^{h\nu/kT_{ex}}$$

recall radiative transfer equation

$$\Delta T_A = T_B - T_{bg} = \frac{h\nu}{k} \left[\frac{1}{e^{h\nu/kT_{ex}}-1} - \frac{1}{e^{h\nu/kT_{bg}}-1} \right]$$

$$\times \left(1 - e^{-\tau}\right)$$

$\tau \gg 1$, neglect T_{bg}

$$\rightarrow T_A = \frac{h\nu/k}{e^{h\nu/kT_{ex}} - 1}$$

↳ determine $T_{ex} = T_k$ from observed T_A

$\tau \ll 1$, neglect T_{bg}

$$T_A = \tau \frac{h\nu}{e^{h\nu/kT_{ex}} - 1}$$

now $\tau = h\nu \phi_\nu [B_{lu} N_l - B_{ul} N_u]/c$

ϕ_ν → line profile function

$$\int \phi_\nu d\nu = 1$$

$$\rightarrow T_A = \frac{hc^2 \phi_\nu}{8\pi k \nu} A_{ul} N_u$$

$$\int T_A dV = \text{const} \times N_u$$

→ determine N_u from line integral

→ τ from N_u

→ T_{ex} from observed T_A, τ
($= T_{min}$)

Problem : LTE often is not a good approximation

(2) LVG - this model is basically the Sobolev approximation (developed for stellar winds) applied to molecular clouds

Main assumption is there are velocity gradients or other motions in the cloud, so that we can treat radiative transfer as a local problem.

(1) Statistical equilibrium

$$n_i(r) \sum_j P_{ij}(r) = \sum_j n_j(r) P_{ji}(r)$$

$$P_{ij} = \begin{cases} A_{ij} + B_{ij} \langle J_{ij}(r) \rangle + C_{ij}(r) & i>j \\ B_{ij} \langle J_{ij}(r) \rangle + C_{ij}(r) & i<j \end{cases}$$

$\langle J_{ij}(r) \rangle$ mean integrated radiation field at necessary frequency

(2) Radiative transfer

$$I = S(1-e^{-\tau}) + I(0)e^{-\tau}$$

$S = j/\kappa$ source function

$$\tau = \int \kappa \, dz$$

$$\langle J_{ij}(r) \rangle = \int_{4\pi} \frac{d\Omega}{4\pi} \int_0^\infty I \phi(\nu') d\nu'$$

$$= (1-\beta) S_{ij} + \beta B(\nu_{ij}, T_{bn})$$

$$\beta = \int_{4\pi} \frac{d\Omega}{4\pi} \int_0^\infty \phi(\nu') e^{-\tau} d\nu'$$

= escape probability of line

need to know $\kappa, j \rightarrow \tau$
$\rightarrow \langle J_{ij} \rangle$

solve (1) + (2) iteratively to get level populations then get T_{ex} from

$$\frac{n_u}{n_\ell} = \frac{g_u}{g_\ell} e^{-\frac{h\nu}{kT_{ex}}}$$

then get T_A from (ie Rayleigh-Jeans limit)

$$T_A = T_{ex}(1 - e^{-\tau})$$

→ compare to observed line strengths

→ vary n, N/dv, T_K until fit

column density / velocity width

→ need several different rotational transitions, maybe in different isotopes, to get well-constrained solution

→ assumes gas has uniform density and temperature

Determining kinetic temperature

(1) $T_K = T_B$ of optically thick, low J

^{12}CO lines

→ 10–20 K if no high-luminosity heat sources

→ T > 40 K in substantial regions of a few clouds w. large heating rates

problems – filling factors, temperature gradients, embedded heat sources, motions → what gas being measured

(2) Level populations of NH_3

→ agree fairly well with CO

problems – optical depth, low angular resolution + sensitivity, only trace dense gas

(3) Level populations of rotational lines of CO, CS, etc → very sensitive if $E_{ul} > kT_{kin}$

→ also get density information

problems – complicated modelling required, observations at different λ

Determining Density

(1) average from N & size or M & size
— $n \sim 5-10 \times 10^3\ cm^{-3}$
- clumpiness → underestimates density

(2) intensities of 2 lines which are not thermalized
- intensity a function of collision rate
- need to know collision rates → only available for a few common molecules
CO, CS, HC_3N
- particular transitions sensitive to small density range
ie CO 1-0 - 2-1 → $10^{2.5} < n < 10^4\ cm^{-3}$

(3) use molecules with high n_{crit}
ie CS, HCN
- crude tracer of high-n gas

Cloud structure → high density clumps in lower density interclump medium

(4) Multi-transition work (basically extension of (2))
- get density and temperature
- very sensitive to n if lines from subthermal regime included, especially if optically thin

problems - complicated models
- collisions rates mostly unknown
- observations at different λ

Determining Column Density

(1) rare isotopes of CO
- optically thin + ubiquitous
- not easy to put >10% of C in CO
- also not easy to deplete it
- low transitions easily excited

^{13}CO + $C^{18}O$

↳ can be optically thick in large clouds

(2) other molecules
- abundance variations make them useless for total (H) column density
- if assume LTE, can get total N for that species
- or use many transitions
- then can compare this to $N(H_2)$ to get absolute abundance

$$\text{eg.}\quad \frac{N(X)}{N(H_2)} = \frac{N(X)}{N(CO)}\,\frac{N(CO)}{A_V}\,\frac{A_V}{N(H_2)}$$

Heyer, Carpenter, & Snell
2001, ApJ, 551, 852

- outer galaxy survey
- 50" resolution + sampling
- ^{12}CO

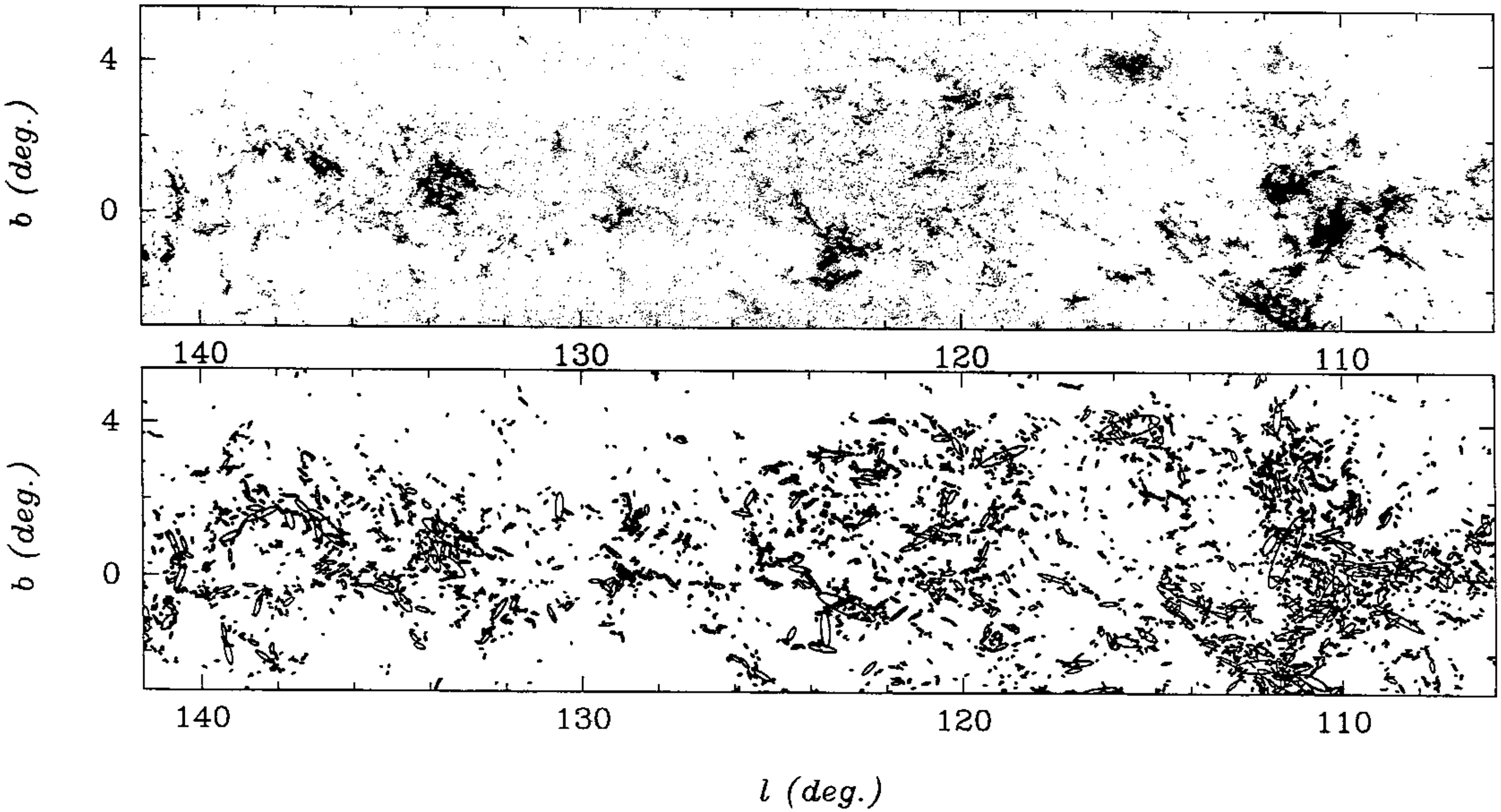

FIG. 1.—*Top:* Image of ^{12}CO $J = 1$–0 integrated intensity over the velocity interval -110 to -20 km s^{-1} from the FCRAO CO Survey of the outer Galaxy (Heyer et al. 1998). The half-tone ranges from 0 (*white*) to 20 (*black*) K km s^{-1}. *Bottom:* Positions, sizes, and orientations of identified objects approximated as ellipses.

lecture 5

$$N(H_2) = 1.9 \times 10^{20}\ I_{CO} \quad (\mathrm{cm}^{-2})$$

$\uparrow X_{CO}$

$$M_{CO} = 4.1\ L_{CO} \quad (M_\odot)$$

$\uparrow$ K km/s pc^2

gravitational parameter

$$\alpha_G \approx \frac{5 \sigma_v^2 r_e}{G M}$$

$\alpha_G \approx 1 \rightarrow$ self-gravitational

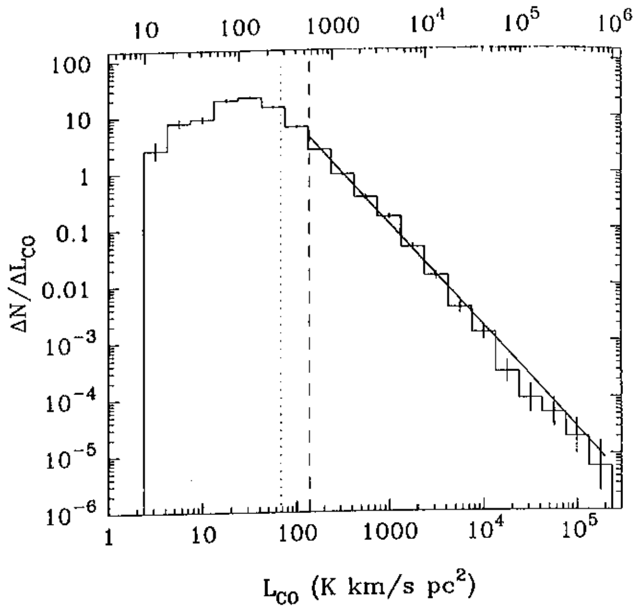

FIG. 3.—CO luminosity function, $\Delta N/\Delta L_{CO}$, for 3901 identified objects. The top x-coordinate shows the corresponding mass scales assuming a constant CO-to-H_2 conversion factor. The vertical dotted line denotes the detection limit of L_{CO}, and the vertical dashed line marks the completeness limit of L_{CO} at a distance of 10 kpc. The power-law fit to bins above the completion limit (*solid line*) is $\Delta N/\Delta L_{CO} \propto L_{CO}^{-1.80\pm0.03}$.

if clouds are <u>not</u> gravitationally bound, then formula <u>overestimates</u> M

can show

$$X_{CO} = 4.1 \left(\frac{\langle T \rangle}{5\,\mathrm{K}}\right)^{-1} \left(\frac{\langle n \rangle}{100\,\mathrm{cm}^{-3}}\right)^{1/2} \alpha_G^{-1/2}$$

[not gravitationally bound $\rightarrow \alpha_G \gg 1$)

$$\frac{\Delta N}{\Delta L_{CO}} = (3.1 \times 10^4)\, L_{CO}^{-1.80}$$

$\rightarrow$ 50% from clouds with $L_{CO} > 7800$ K km/s pc^2

velocity dispersion σ_v

- → thermal
- → turbulent
- → rotational
- → expanding motions

σ_v increases with r_e for $r_e > 7\,pc$

BUT no trend for $r_e < 7\,pc$

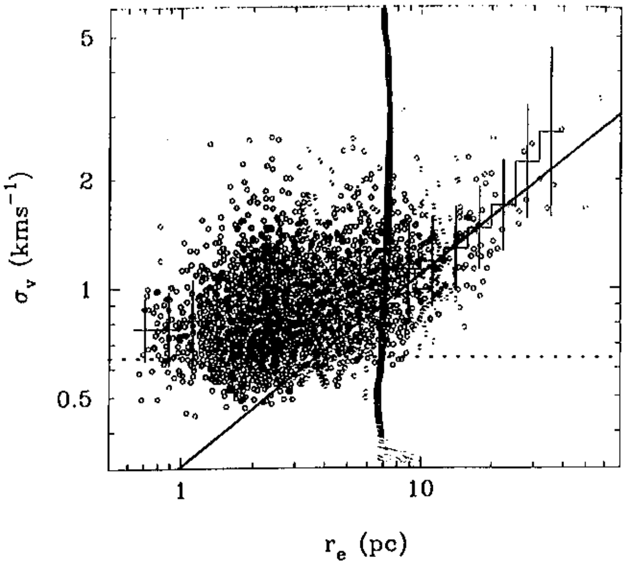

FIG. 6.—Variation of measured velocity dispersion, σ_v, and effective size, r_e. The thin solid line shows the mean value within logarithmic bins of r_e, and the error bars reflect the dispersion of values about the mean in each bin. The thick solid line shows the power-law fit to the clouds with $r_e > 9$ pc. The slope of the power law is similar to that found by Solomon et al. (1987). The horizontal dashed line shows the velocity dispersion to which the measured values are accurate to within 15%.

$$M_{vir} = \frac{5\sigma_v^2 r_e}{G}$$

$$\alpha_G = \frac{M_{vir}}{M_{CO}} = 53\,L_{CO}^{-0.5}$$

- only most luminous clouds have $\alpha_G \sim 1$

⇒ smaller clouds are internally overpressured with respect to gravity

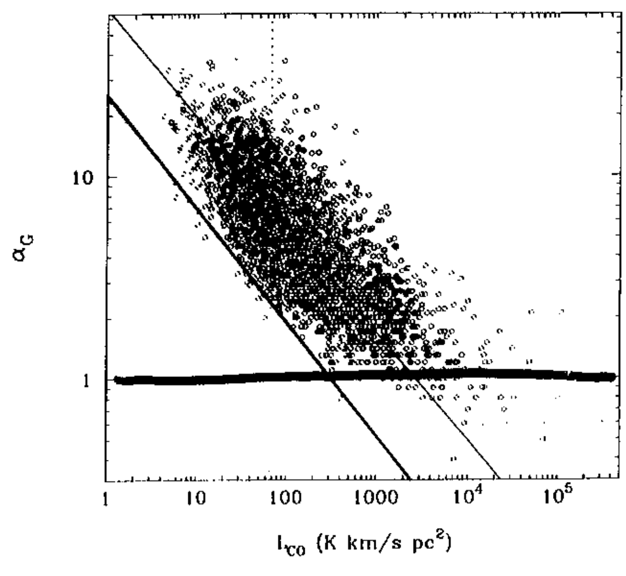

FIG. 7.—Variation of the gravitational parameter, α_G, with CO luminosity. The dotted vertical line denotes the detection limit of L_{CO} at a distance of 10 kpc. The thick solid line shows the minimum value of α_G to which the decomposition is sensitive as a result of the observational selection effect that excludes narrow-line clouds.

regions with large α_G must be either

- short lived, or
- bound by external pressure

$t_{dyn} \sim \frac{l_{min}}{2\sigma_v} \sim 5-50 \times 10^4 \, yr$

$\ll t_{chem} > 10^6 \, yr$

more likely pressure bounded

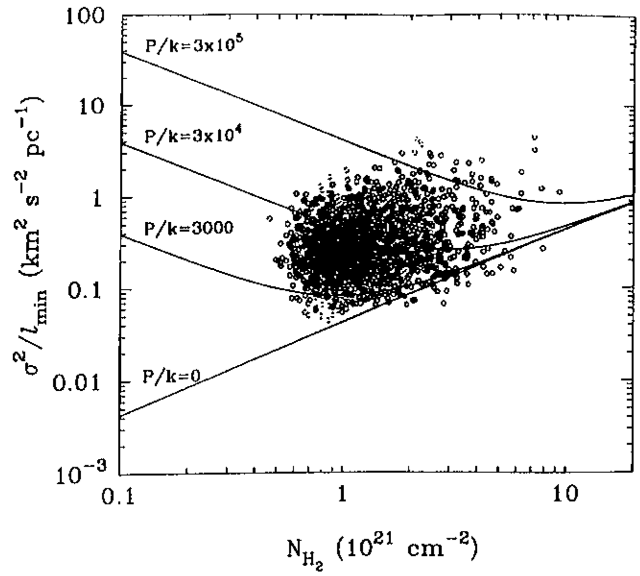

FIG. 11.—Values of σ_v^2/l_{min} vs. the mean column density for the identified objects. The solid lines show the variation of this value for varying external pressures for bound objects.

Virial theorem:

$$\frac{\sigma_v^2}{l_{min}} = \frac{P_0}{k} \frac{k}{m_{H_2}} \frac{1}{N_{H_2}} + \frac{\pi G m_{H_2}}{5} N_{H_2}$$

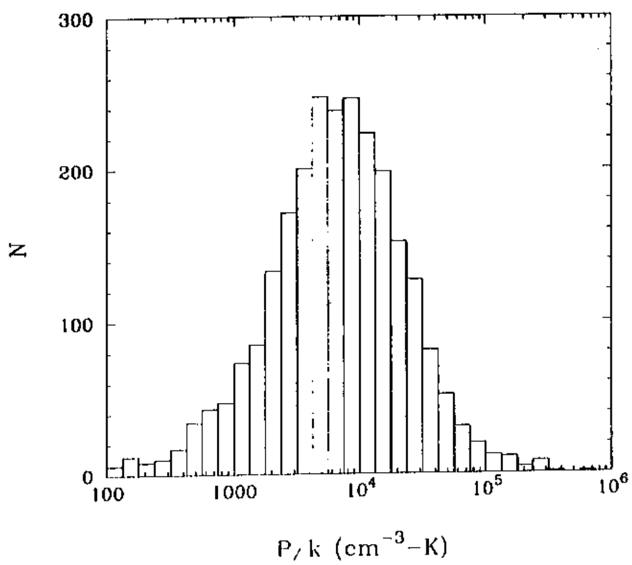

FIG. 12.—Distribution of required external pressures to bind the internal motions of identified molecular regions.

for observed σ_v^2/l, mean pressure $\sim 1.4 \times 10^4$ K/cm^3

most likely source of this pressure is weight of overlying layer of atomic gas

need $N_H \sim 2 \times 10^{21}$ cm^{-2} to shield H_2

GMC Lifetimes: Still Unresolved

(1) Long lifetimes ($> 10^8$ yr) (Scoville + Sanders 1987)

- substantial numbers of GMCs in interarm regions
  - → lifetimes longer than time between spiral arm passages
- also z scale-height decreases with increasing cloud mass
  - → equipartition of GMC kinetic energy
  - → survive several cloud-cloud collision times

(2) short lifetimes (few $\times 10^7$ yr) (Elmegreen 1985 PPII)

- from star cluster ages + cloud statistics

$$\langle t_{cloud} \rangle = t_{cluster} \left(1 + \underbrace{\frac{N_{with\ cluster}}{N_{without\ cluster}}}_{\sim 1} \right)$$

- ages of OB associations $\sim 10^7$ yr

GMC lifetimes: approaching concensus?

① short estimates ~10 Myr (ie Elmegreen 2000, ApJ)
- based on age spread of young stars ie $\lesssim 10$ Myr for OB association
→ star formation in 1-2 × $t_{cross} = \frac{R}{\sigma_v}$

② long estimates ~100 Myr (ie Scoville & Wilson 2004, conf. proceedings)
- mass conservation on Galactic orbit implies

$$\frac{M_{H_2}}{\tau_{H_2}} = \frac{M_{HI}}{\tau_{HI}}$$

$M_{H_2} > M_{HI}$ in inner disk

τ_{HI} = smaller of
- arm to arm transit time
- $t_{dynamical}$ ($n \sim 10$ cm^{-3})

$\Rightarrow \tau_{HI} > 5 \times 10^7$ yr $\Longrightarrow \tau_{H_2} \gtrsim 10^8$ yr

(Note $\tau_{H_2} \neq$ GMC lifetime necessarily)

③ lifetimes ~30 Myr from theory (Williams & McKee 1997) and observations (Engargiola et. al. 2003; Rosolowsky 2005, PhD)

Theory: 10^6 $M_\odot$ cloud destroyed in 30 Myr by photoevaporation by O stars

Observations: association with HI filaments, HII regions

Why are the column densities of GMCs roughly constant?

4. theories

1. N is near but below critical value for support by $\vec{B}$ fields (Shu et al ARAA <u>25</u>, 23 (1987))

2. Clouds are in equilibrium with external pressure (Elmegreen 1989 ApJ <u>338</u>, 178)

$$P_{ext} \sim \frac{GM^2}{R^4} \propto N^2$$

3. "Photoionization regulated star formation" (McKee 1989 ApJ <u>345</u>, 782)
   - time scale for ambipolar diffusion $\propto X_e$
   - low mass star formation only possible if X_e low
   - diffuse cloud contracts quickly to $A_V \sim 4$, central parts shield, t_{ad} drops, star formation starts
   - outflows stabilize cloud → column densities of most clouds near onset value

4. No physical basis → due to observational bias + sensitivity limits eg Kegel 1989 AA <u>225</u>, 517